Measurements of CCE with pad sensors with a low intensity electron beam

P. Grutta, University of Padua and INFN

Padua, 11/01/24

Table of contents

Scientific context and scope

- The **scientific context** is LUXE's R&D campaign to design and characterize a radiation-hard sapphire radiation detector for high-energy Compton beam monitoring. The typical beam conditions at LUXE is a bunch of 10^9 16 GeV photons, distributed over 2x2 cm^2.

- The **scope** for the Frascati-BTF 9-11 May 2022 is **characterization** of the **response** of a simplified sapphire '**pad**' **sensor** (prototype). This is quantified by the ***charge collection efficiency***

$$CCE \equiv \frac{Q_{collected}}{Q_{ionisation}}$$

  defined as the ratio between the collected charge and the charge created by ionization by the incident radiation.

- The CCE is measured as a function of both the external biasing HV and the bunch charge of the electron beam – that is ***CCE(V)*** and ***CCE(Q)***.

Experimental setup. Beam

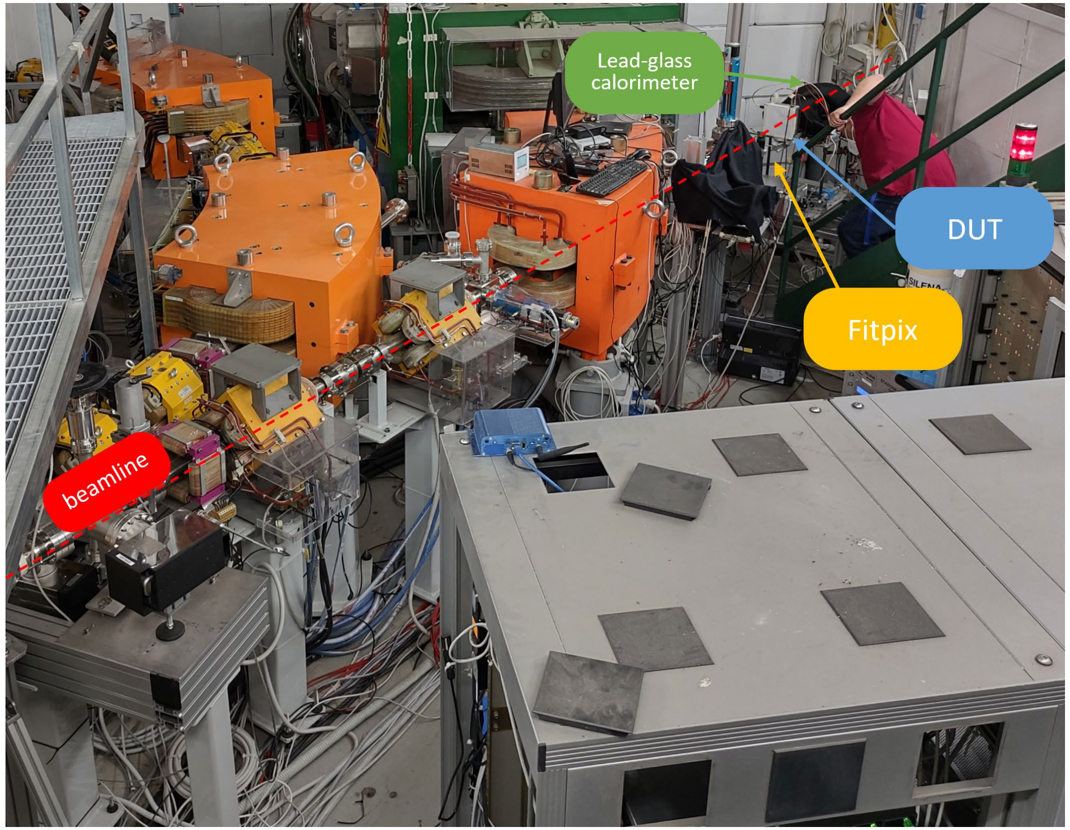

Figure 1.

- Beam Test Facility (BTF) at INFN Frascati National Laboratories used in **parasitic mode** in BTF1-hall.
- The typical beam setup had
  - a bunched 10Hz e^- beam;
  - energy of 300MeV;
  - xy-profile gaussian with typical sigma of

$$(\sigma_x, \sigma_y) = (2.1, 1.8)\ mm$$

- A FitPix silicon detector measures the **beam shape**.
- A lead-glass calorimeter measures the **beam energy**.

Experimental setup. DUT

- Stack of 2 identical PCB, separated by 2cm
  - Sapphire detector (top)
  - 2x amplifiers (bottom)

- With respect to the beam, we have:
  - upstream PCB with 110um sapphire.
  - downstream PCB with 150um sapphire.

- The front cover is replaced with a thin Al-foil (for EM shielding) to reduce e-beam secondary showers. There is no beam exit window.

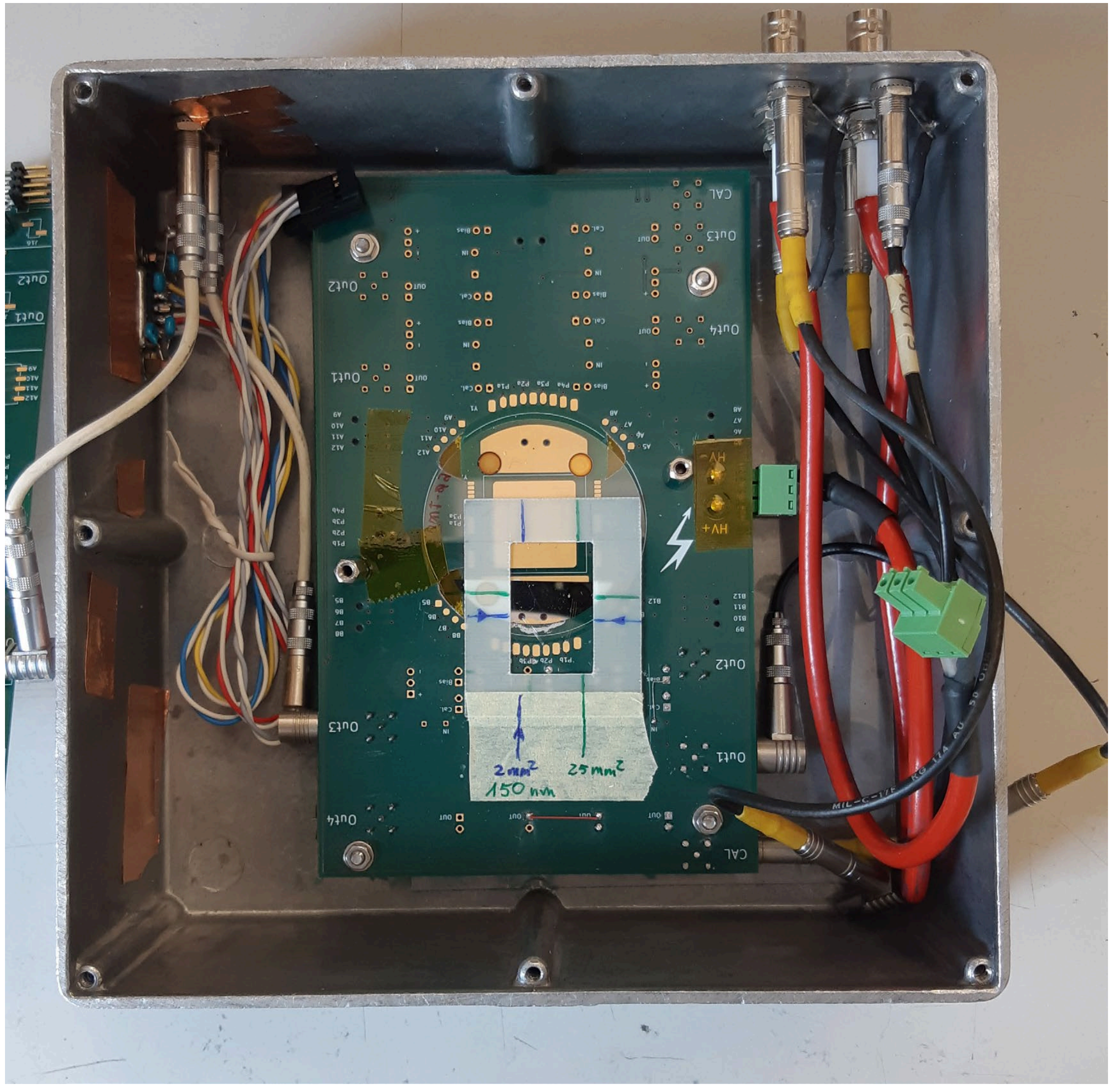

Figure 2.

Experimental setup. Sapphire sensors

- Single crystal 2-inch ($d = 50.8\text{mm}$) sapphire wafer <0001> double-side polished, with thickness:
  - 110um (Situs GmbH, *Germany*) and
  - 150um (UniversityWafers, *USA*).
- Top surface is metallized with a 4 pads, with small (large) pads of $r_{SP} = 0.8\text{mm}$ ($r_{LP} = 2.75\text{mm}$).
- Bottom surface is metallized with a ground plane with half-moon shape.
- The two pads 2, 4 are wire-bonded to the PCB and connected to the amplifiers.

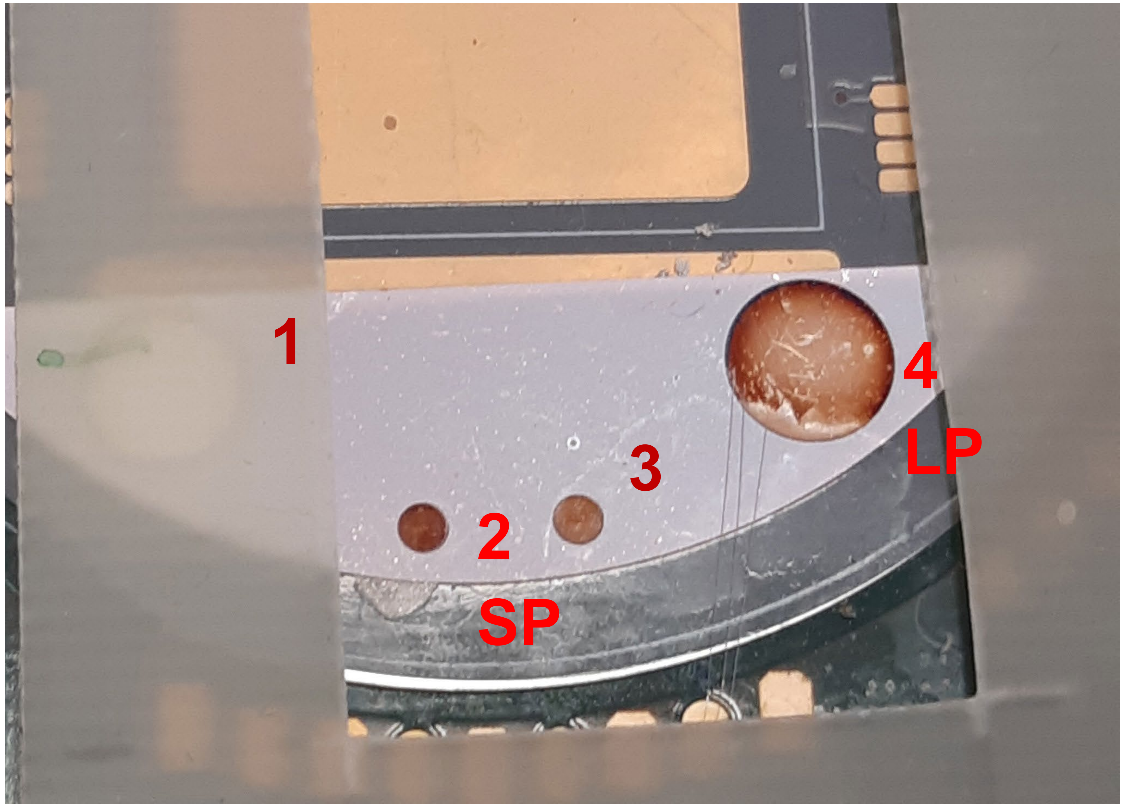

Figure 3. Picture of the 110um sensor after wire-bonding of the large pad.

Readout and Methodology

$$CCE \equiv \frac{Q_{collected}}{Q_{ionisation}}$$

- Each pad LP/SP is routed to an independent 200mV/fC charge sensitive amplifier and signal readout of **charge collected** is done with a digital oscilloscope.
- The **charge deposited** is calculated (Geant4) from the e.dep. in the pad cylindrical volume ($Q_{dep} = \frac{E_{dep}}{27eV} \cdot e$), neglecting hole charge (as in the literature).
- Beam-related systematics are evaluated with a Geant4-MC.
- Charge collection the E-field fringes is estimated with an Allpix2 MC simulation:
  - negligible (3%) for the LP;
  - important (7-16%) for SP.
- **High-voltage** scan in the range
  - $V_{bias} \in [0, 800]$ V, with sparks at higher V.
- **Beam-charge** scan in the regions
  - up to 8ke/bunch at 100V;
  - up to 80ke/bunch at 0V.,

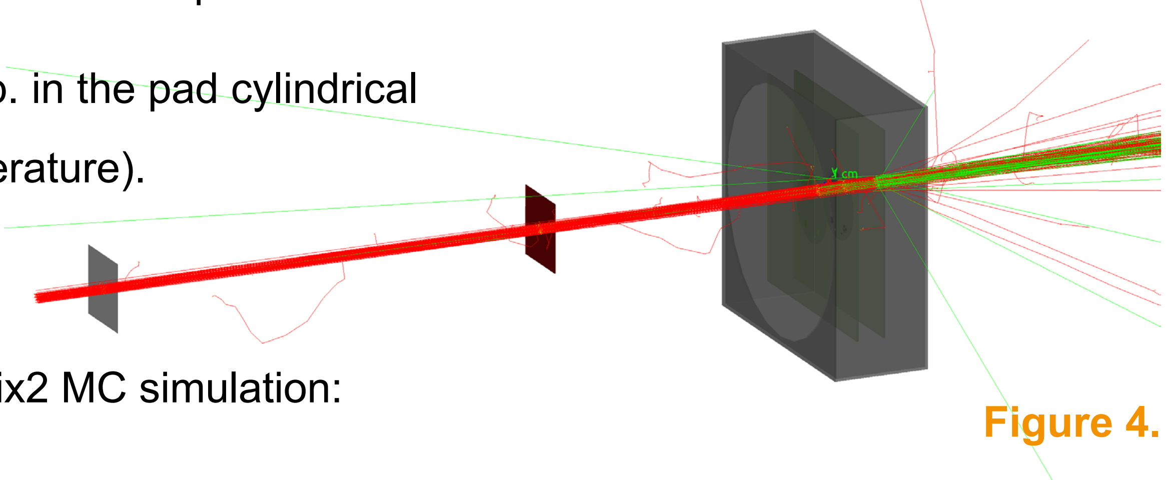

Figure 4.

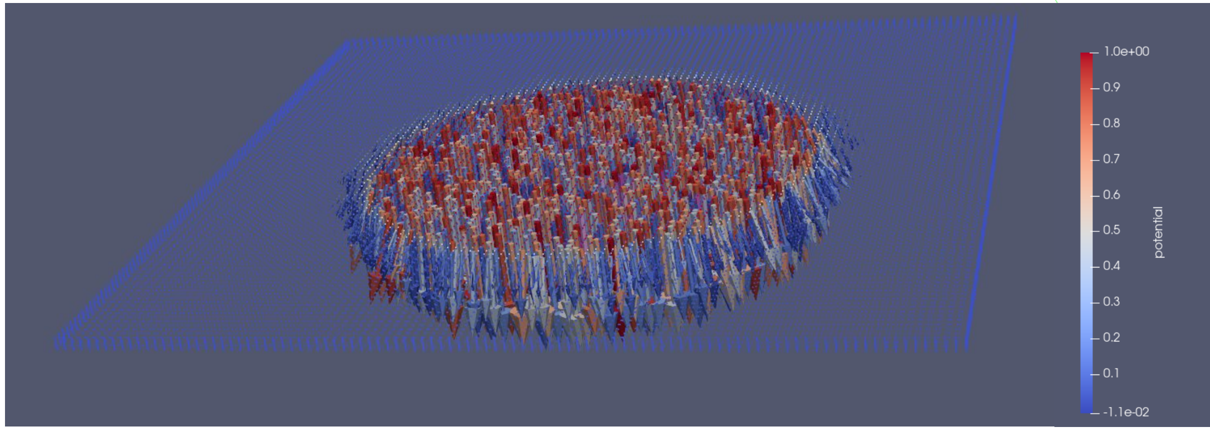

Figure 5. Electric field vector in the large pad for $V_{bias} = 100\text{V}$

Analysis. Theory

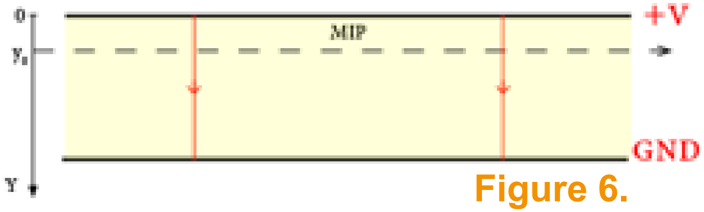

Figure 6.

- If we assume the following conditions to hold
  - The detector is planar (thickness d is negligible compared to other dimensions)
  - The transport properties and the electric field are uniform in whole volume of the sensor.
  - The free charge in stationary conditions is negligible and its generation, due to a photon (or a particle) absorption, is instantaneous.
  - Diffusion and detrapping phenomena are negligible and the number density of charge carries decrease with time as $\sim e^{-t/\tau}$.

The CCE contribution from a localized initial charge deposited at y_0 is

$$\mathrm{CCE}_e(y_0) = -\frac{f_d}{d} \cdot \int_{y_0}^{0} dy\, e^{-\frac{y-y_0}{(\mu\tau)_e E_0}} = -V\, f_d\, \frac{(\mu\tau)_e}{d^2} \left(1 - e^{\frac{y_0}{(\mu\tau)_e E_0}}\right) \qquad (15)$$

$$\mathrm{CCE}_h(y_0) = \frac{f_d}{d} \cdot \int_{y_0}^{d} dy\, e^{-\frac{y-y_0}{(\mu\tau)_h E_0}} = V\, f_d\, \frac{(\mu\tau)_h}{d^2} \left(1 - e^{-\frac{d-y_0}{(\mu\tau)_h E_0}}\right) \qquad (16)$$

If a uniform distribution of charge along a track (i.e., the MIP case) is considered, by integrating (15)+(16) over the thickness y_0 we get the CCE(V) we are looking for

$$\mathrm{CCE}(V) = f_d\, k \left[1 + k\left(\exp\left(-\frac{1}{k}\right) - 1\right)\right]$$

- $f_d \in [0,1]$ – the effective fraction of pairs propagating in sapphire;
- with $k \equiv \frac{\mu_e \tau_e}{d^2} V$

Analysis. Theory

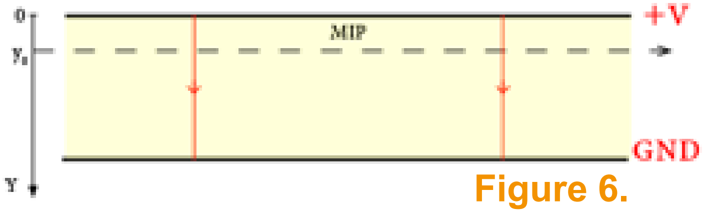

Figure 6.

- If we assume the following conditions to hold
  - The detector is planar (thickness d is negligible compared to other dimensions)
  - The transport properties and the electric field are uniform in whole volume of the sensor.
  - The free charge in stationary conditions is negligible and its generation, due to a photon (or a particle) absorption, is instantaneous.
  - Diffusion and detrapping phenomena are negligible and the number density of charge carries decrease with time as $\sim e^{-t/\tau}$.

The CCE contribution from a localized initial charge deposited

If a uniform distribution of charge along a track (i.e., the MIP c thickness y_0 we get the CCE(V) we are looking for

$$\mathrm{CCE}(V) = f_d\, k\left[1 + k\left(\exp\left(-\frac{1}{k}\right) - 1\right)\right]$$

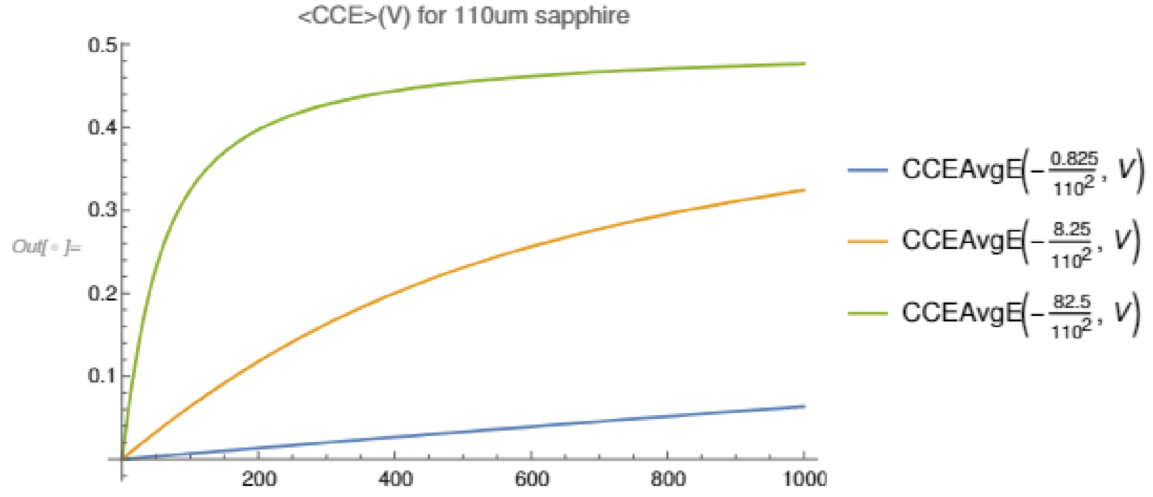

Figure 7. Plot of $\mathrm{CCE}\left(\frac{\mu\tau}{d^2}, V\right)$ for a 110um planar detector with $-(\mu\tau)$ products of 0.825, 8.25, 82.5 $\mathrm{um}^2\mathrm{V}^{-1}$ and $f_d = 1$.

Analysis. CCE(V)

- Short runs of 1k events at low beam charge (500e) scanning the HV in 100V steps.

- **Results**
  - Typical efficiency of 14% (12%) for the 110µm (150µm) at 1kV.
  - Typical charge carriers drift distance small w.r.t. the sensor thickness (*linear regime* of the CCE(V) eq.).
  - The $(\mu\tau)_e$ product is extracted from the fit:
    - ► for the 110µm $(\mu\tau)_e \in [1.6, 2.4]\ \mathrm{\mu m^2 V^{-1}}$
    - ► for the 150µm $(\mu\tau)_e \in [2.4, 3.1]\ \mathrm{\mu m^2 V^{-1}}$

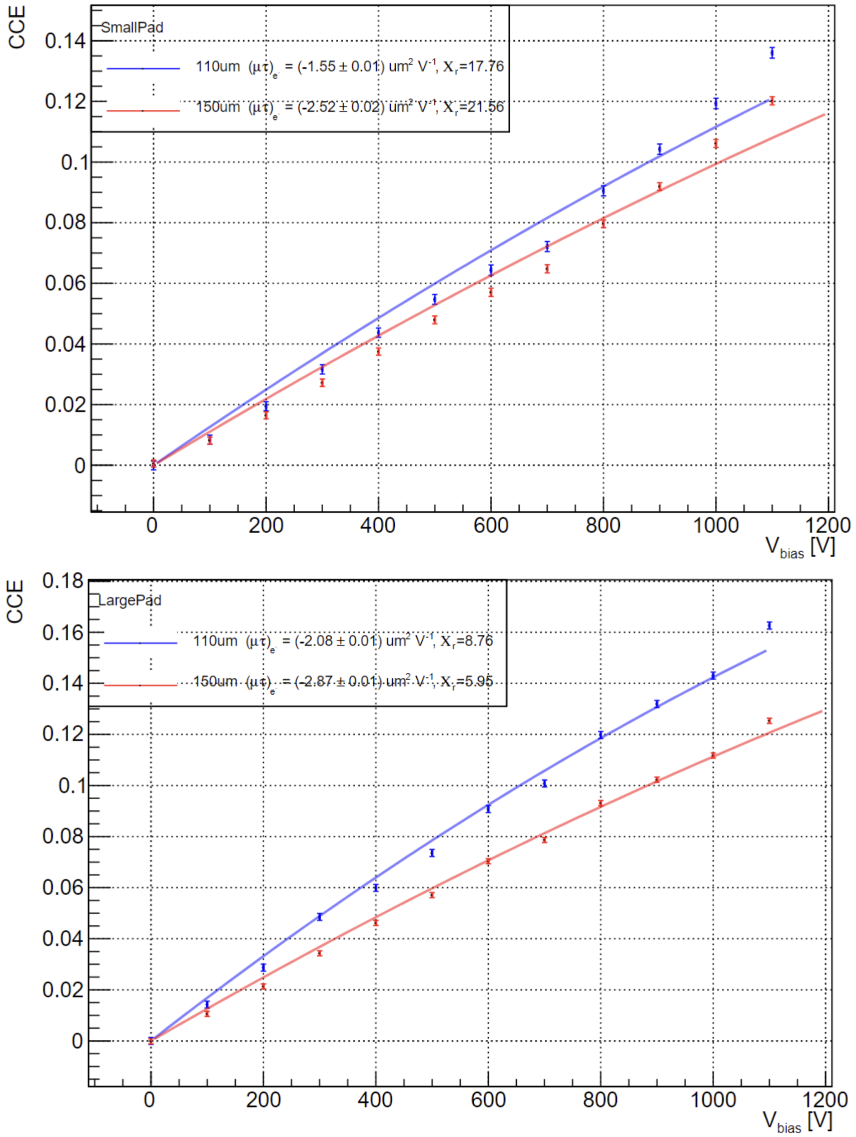

Figure 7. Top: small pad. Bottom: large pad.

Analysis. CCE(Q)

- Short runs of 1k events at low beam charge (500e) scanning the HV in 100V steps.

- **Results**
  - Typical efficiency of 14% (12%) for the 110µm (150µm) at 1kV.
  - Typical charge carriers drift distance small w.r.t. the sensor thickness (*linear regime* of the CCE(V) eq.).
  - The $(\mu\tau)_e$ product is extracted from the fit:
    - ► for the 110µm $(\mu\tau)_e \in [1.6, 2.4]\ \mu\mathrm{m}^2\mathrm{V}^{-1}$
    - ► for the 150µm $(\mu\tau)_e \in [2.4, 3.1]\ \mu\mathrm{m}^2\mathrm{V}^{-1}$
  - Linear dependence of CCE with beam bunch charge up to 40k e/bunch.

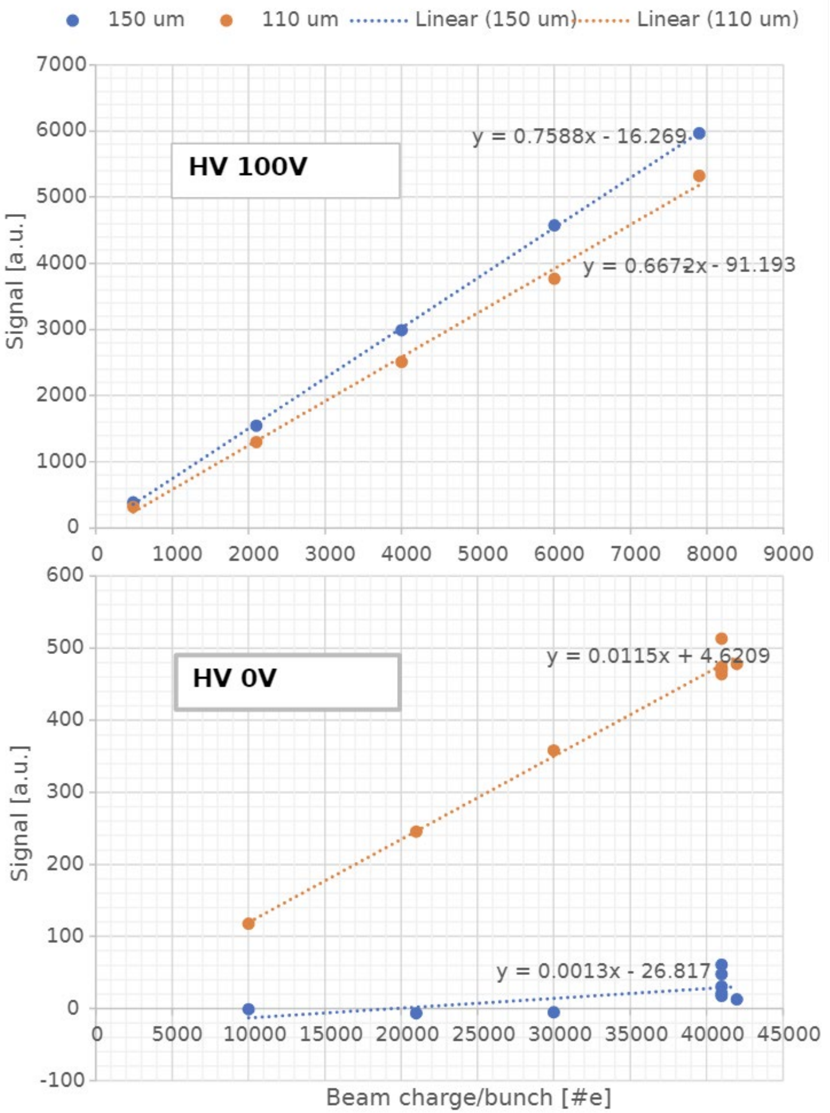

Figure 8. Collected charge (large pad) as a function of the beam charge. Top: at HV =100V. Bottom: at HV=0V.

Analysis. Summary for (μτ)

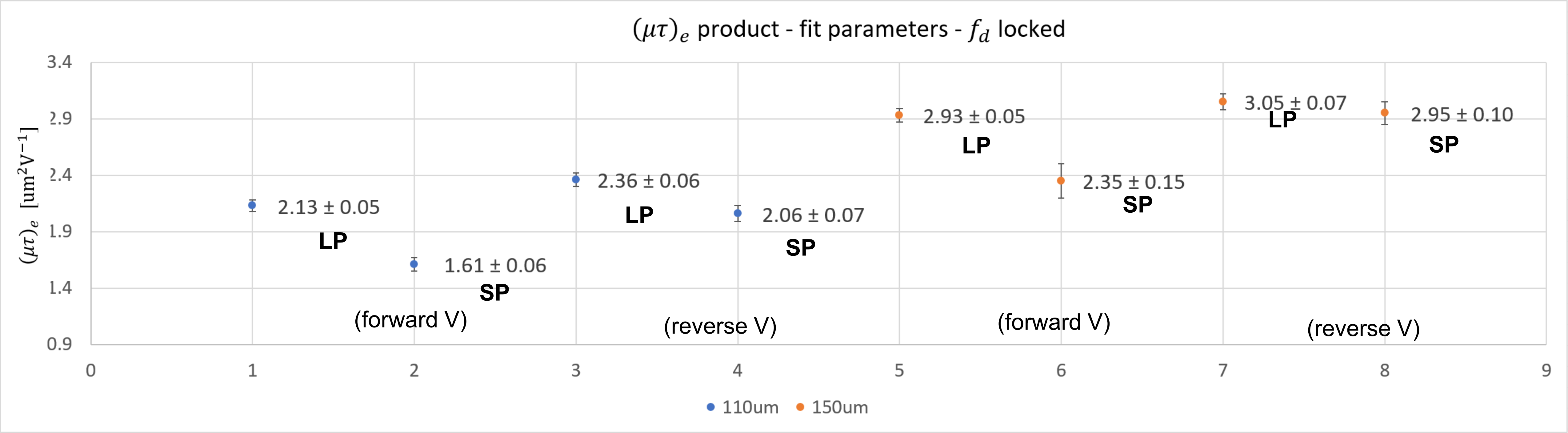

- Large systematics → in the other TBs beam monitoring DAQ has been implemented.
- There are differences with respect to the literature [DOI 10.1088/1748-0221/10/08/P08008]:
  - the CCE (at equal E-field) of the samples does not vary much (2-3%) but is small (i.e., the 10% reported);
  - the extracted $(\mu\tau)_e$ in the range $[1.6, 3.1]$ μm^2V^{-1} are one order of magnitude smaller;

Conclusions and open points

- Hints of **residual field** in the 110um-thick detector (slide 11).
- Typical CCE of 13% (10%) at 1kV for 110um (150um) sensor.
- Higher CCE for the 150um for any given E-field (V/um).
- The CCE with reverse bias (pad at GND) are higher (2-3%). Why?

backup

Experimental setup. Geometry

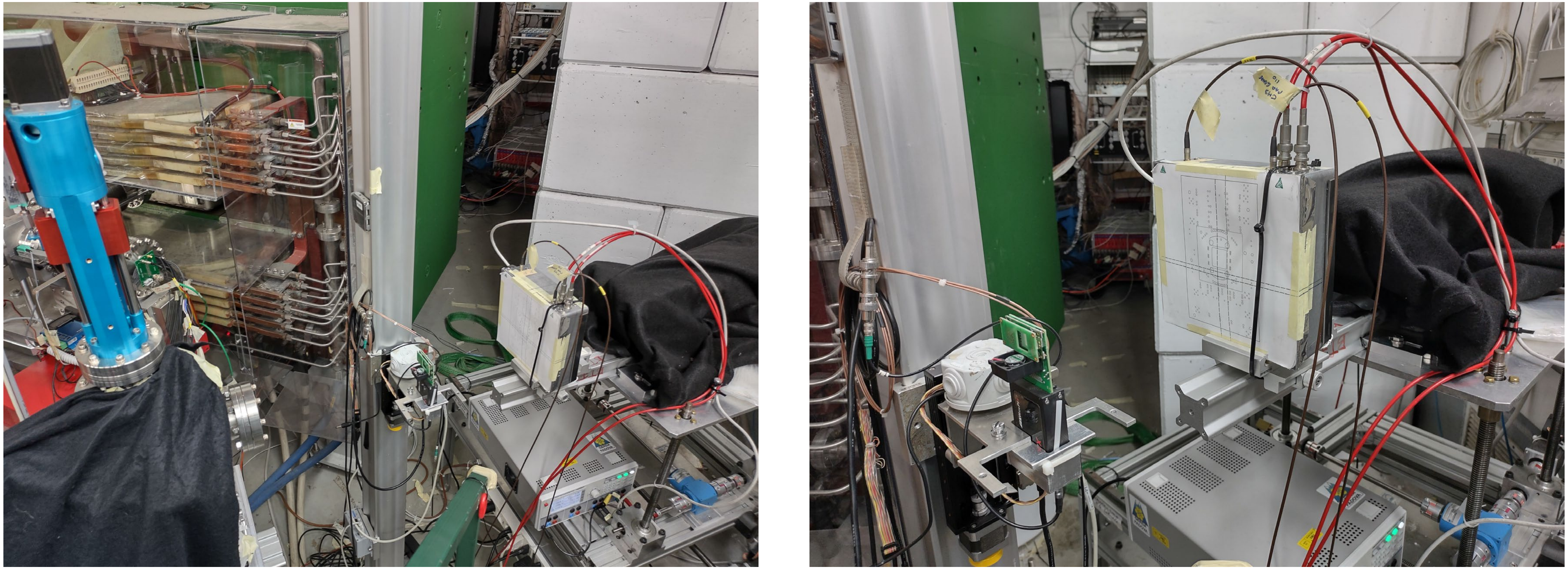

Figure 2. Placement of the detectors along the beam line. Left: from right to left of: the 50 um Ti-window terminating the beam-pipe; 33 cm of air; silicon vertex detector (fitpix); 22 cm of air; DUT; 10 cm of air; lead-glass calorimeter. Right: the DUT assembly in its final position on the movable table.

Analysis. CCE(V) – reverse V_{bias}

- High-voltage scans from 0 to 1.1kV with a gaussian beam $(\sigma_x, \sigma_y) = (2, 1.8)\ \mathrm{mm}$ with avg. beam multiplicity (bunch charge) of 500e and 1000e. Small runs of 1k events to accommodate DAQ and minimize beam position drift systematics.
- The $(\mu\tau)_e$ product is extracted from the fit being
  - for the 110um $(\mu\tau)_e \in\ [1.6, 2.4]\ \mathrm{um}^2\mathrm{V}^{-1}$
  - for the 150um $(\mu\tau)_e \in\ [2.4, 3.1]\ \mu\mathrm{m}^2\mathrm{V}^{-1}$
- Same analysis with reverse bias (pad@-V)

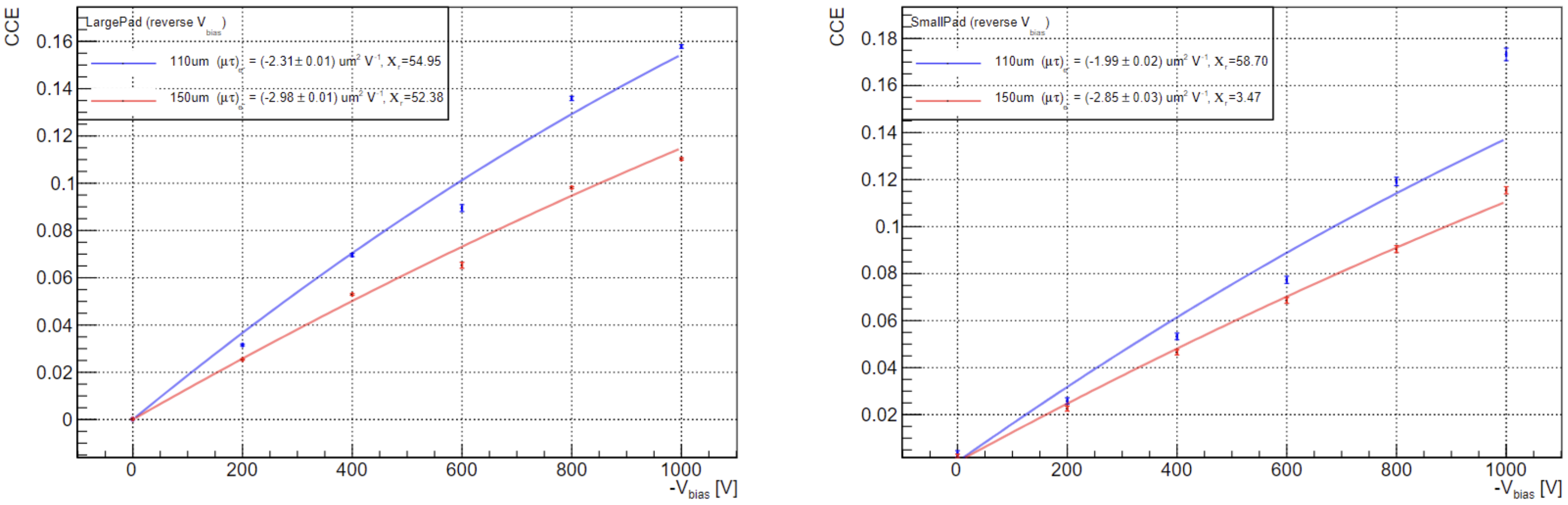

(a) Large Pad (b) Small Pad

Figure 16: Scan of the charge collection efficiency as a function of the reverse biasing voltage $-V_{\text{bias}}$. Statistical uncertainties are attached to data points. Left: CCE for the large pad (r=2.75mm). Right: CCE for small pad (r=0.8mm). Blue (red) line color for the 110um (150um) wafer.

Experimental tests

1. Sapphire wafers characterization
2. Test beams

Experimental campaigns

- A long experimental campaign, starting since May 2022, *is ongoing* to investigate sapphire properties as radiation detector, from prototypes (pad-sensor, 4-strip) to the present GBP design.
- Sapphire wafers quality control and characterization.
- Test beams. Experimental activity and support from simulations:
  - TB1-pad at INFN BTF (Frascati, Italy) CCE and Allpix^2 for fringe effects;
  - TB2-4 strip at CLEAR (CERN) evaluation of the CCE and accumulated dose from an electron beam;
  - TB3-192, TB4-192, TB5-192 evaluation of deposited charge for CCE calculation. Estimate of systematic uncertainties.

Sapphire pads
(May 22, INFN-LNF)

Sapphire 4-strip
(Sep. 22, CERN)

Sapphire (Tomsk) 192-strip
(Mar. 23, CERN)

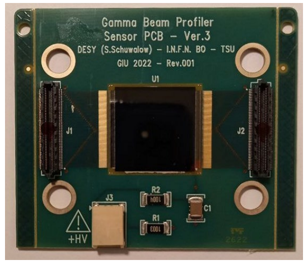

Sapphire (FBK) 192-strip
(Jun. 23-today CERN)

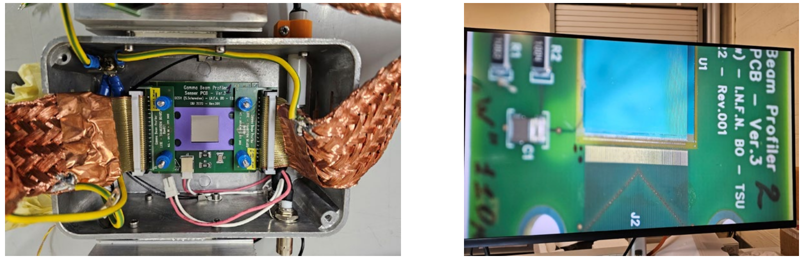

Sapphire wafers quality control and characterization

- Sapphire from several manufacturers tested
  - 4x150µm from UniversityWafer Inc. (USA)
  - 3x110µm from Wuppertal (Germany)
- Optical and electron microscopy are used to inspect the samples to characterize the metallization: **sizes**, **thickness**, **composition** and defects

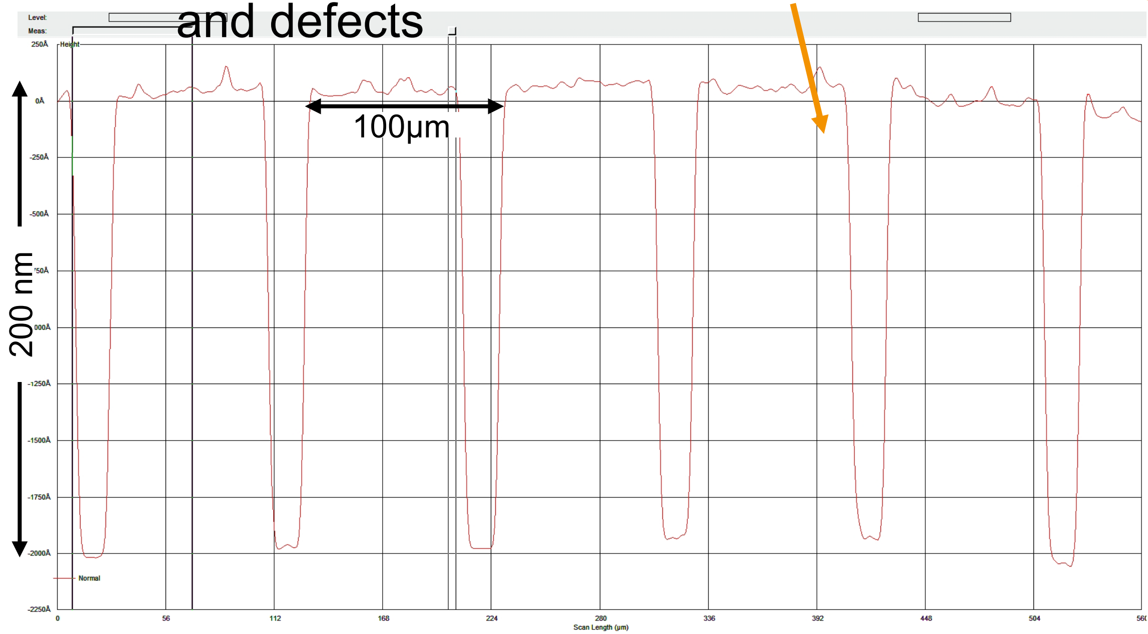

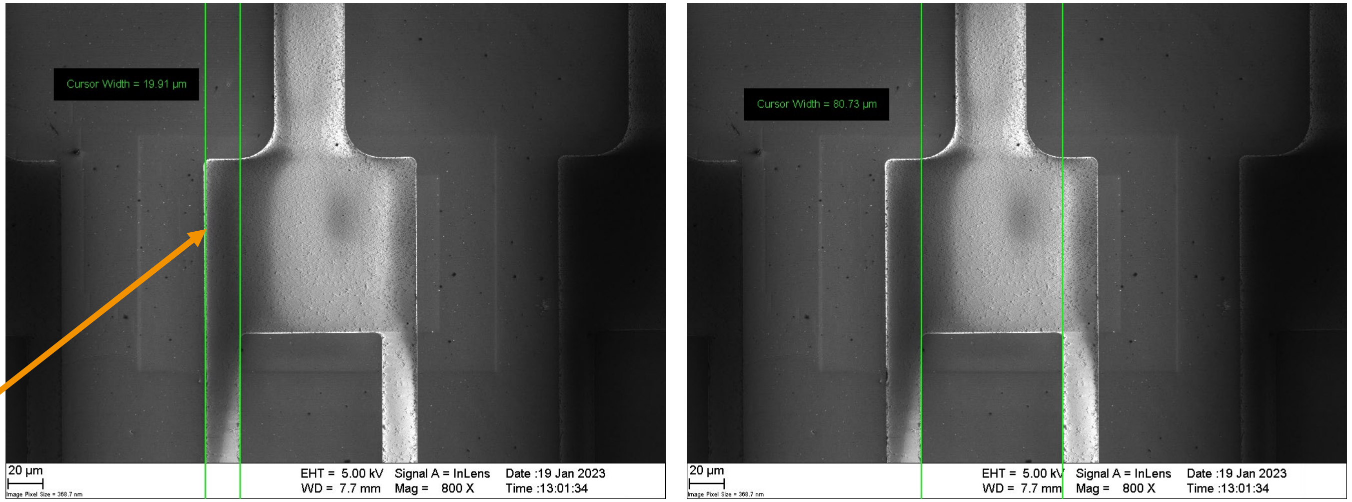

Strip XRD spectrum

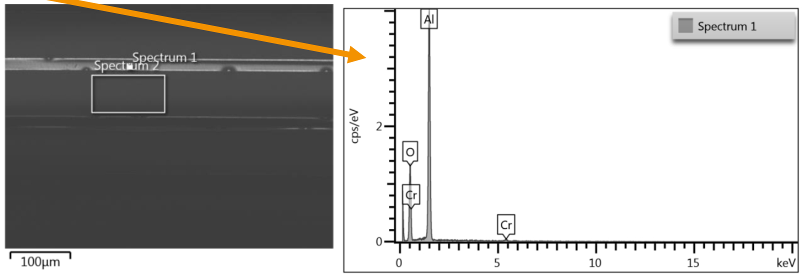

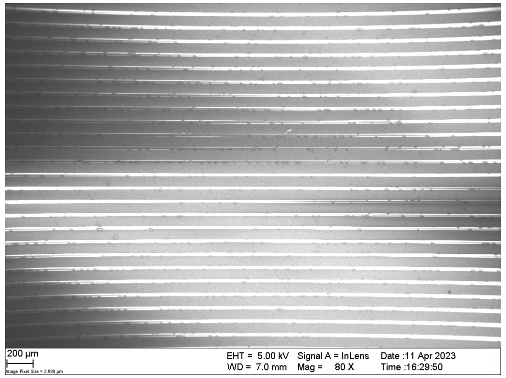

Backside layer XRD spectrum*

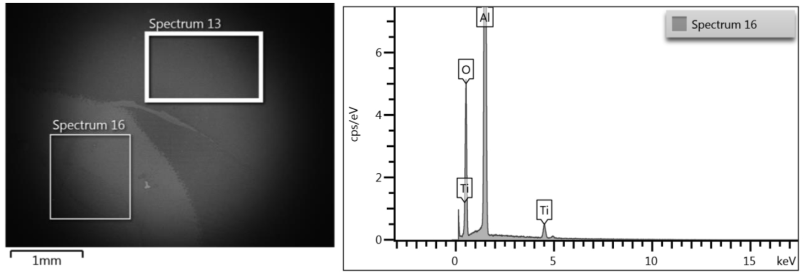

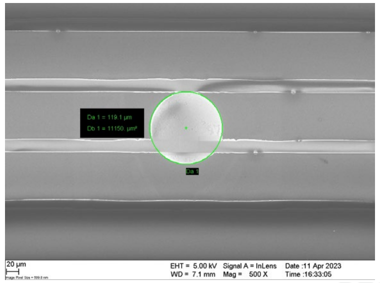

There is no difference between spectra 13 and 16. So, spectrum 16 has been shown only.

Test beams: rationale, challenges, progresses

- **Objectives** outline of the test beams:
  1. Charge collection efficiency (CCE) as a function of the biasing voltage → **CCE(V)** *pad-sensor*
  2. CCE(V), strip uniformity & relative eff. as a function of the absorbed dose → **rad.-damage** *4-strip*
  3. **Electronics system test** (PSU, FERS) with the final detector design *192-strip*

- Several **challenges faced** early tests (i.e., data synchronization, small 4-strip w.r.t. the beam leading to large systematic errors, beam stability, etc.) led to improve the experimental setup by
  - early daq-software development for *acquisition* and data *monitoring.*
  - Design and development of an ancillary system – i.e., based on a ‘scintillator & camera’ setup - allowing for a shot-to-shot acquisition/monitor of facility’s beam characteristics (spatial profile and charge).

Sapphire pads
(May 22, INFN-LNF)

→

Sapphire 4-strip
(Sep. 22, CERN)

→

Sapphire 192-strip
(Mar. 23, CERN)

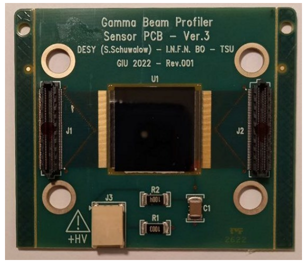

Test beams: Pad sensor test at Frascati INFN national laboratories

- **Goals**
  - Investigate sapphire CCE as a function of the **external biasing voltage**
  - and **beam bunch charge**.

- **Setup**
  - 2-inch sapphire wafer with two metal-plated pads ($r_{SP} = 0.8\text{mm}$, $r_{LP} = 2.75\text{mm}$) on top surface. Two samples (thickness 110µm, 150µm) stacked one after the other in the DUT assembly.
  - Strip LP/SP routed to independent 200mV/fC charge sensitive amplifiers and signal readout with a digital oscilloscope.
  - In-air test with a 300MeV bunched e-beam (1-10^5 e/bunch, 10ns) monitored with a 400µm-thick silicon GP (upstream) and lead-glass calorimeter

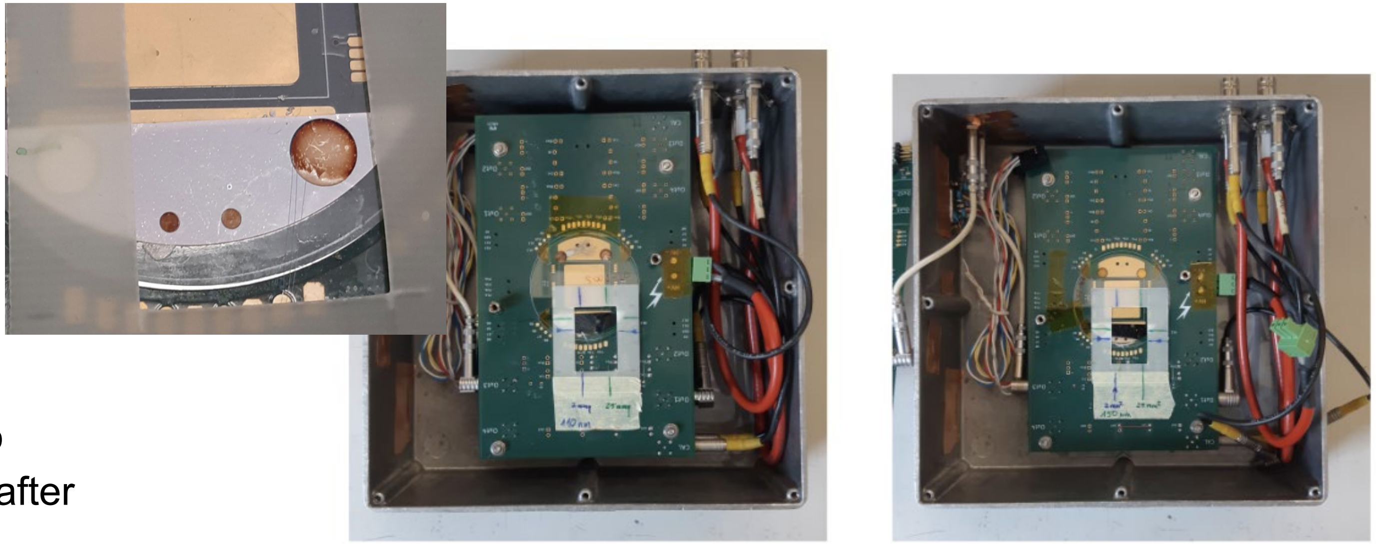
(a) upstream (110) (b) downstream (150)

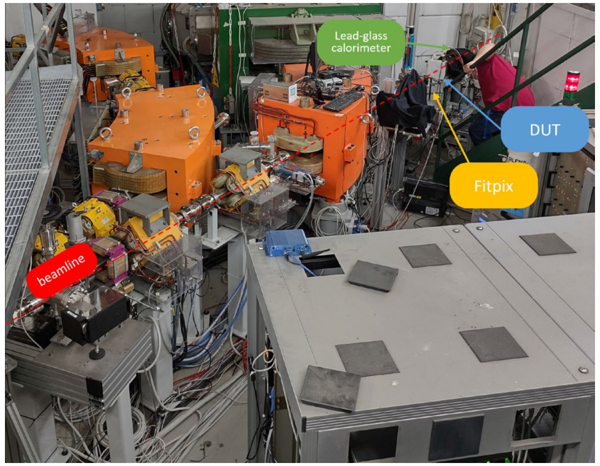

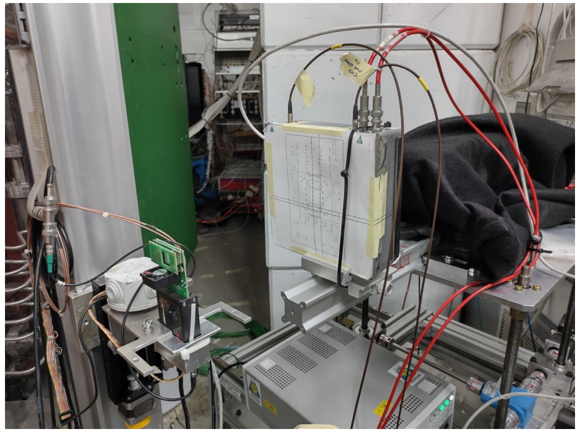

Test beams: Pad sensor test at Frascati INFN national laboratories

- **Challenges**
  - Large systematic uncertainties from beam-DUT misalignments and air scatterings – evaluated by a Geant4 sim.
  - Beam profile and charge not acquired – average values over 1k bunches used.

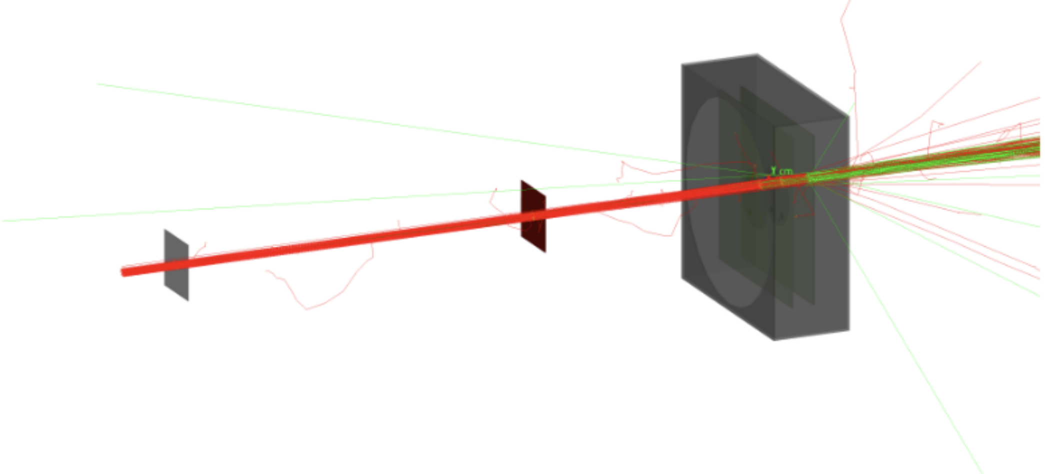

Figure 11: GEANT4 visualization of the test beam geometry for a few electrons. From left to right, along the beam line direction: 50um Ti beam pipe exit window, air, profilometer, air, DUT. Color code is the following: red/green/blue lines for electrons/photons/positrons.

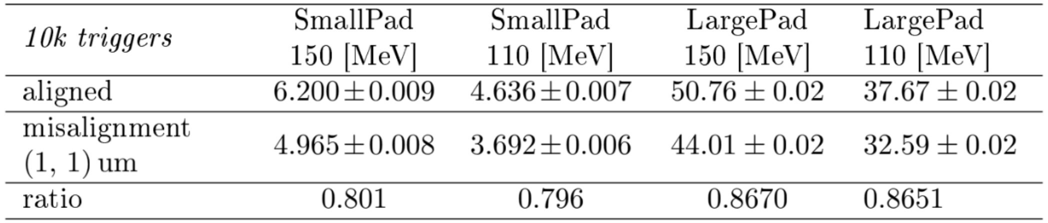

10k triggers	SmallPad 150 [MeV]	SmallPad 110 [MeV]	LargePad 150 [MeV]	LargePad 110 [MeV]
aligned	6.200 ± 0.009	4.636 ± 0.007	50.76 ± 0.02	37.67 ± 0.02
misalignment (1, 1) um	4.965 ± 0.008	3.692 ± 0.006	44.01 ± 0.02	32.59 ± 0.02
ratio	0.801	0.796	0.8670	0.8651

Table 2: Energy deposited in the pads of sapphire sensors when beam center is perfectly aligned, and when a (1, 1) mm misalignment is present. Typical beam profile parameters have been used: $(\sigma_x, \sigma_y) = (2.13, 1.87)$ mm and multiplicity $N = 1000$. Simulation statistics is 10k triggers.

Test beams: Pad sensor test at Frascati INFN national laboratories

Challenges

- Large systematic uncertainties from beam-DUT misalignments and air scatterings – evaluated by a Geant4 sim.
- Beam profile and charge not acquired – average values over 1k bunches used.

Results

- Typical efficiency of 14% (12%) for the 110µm (150µm) operating at 1kV.
- Typical charge carriers drift distance small w.r.t. the sensor thickness.
- Linear dependence of CCE with beam bunch charge up to 9k e/bunch.

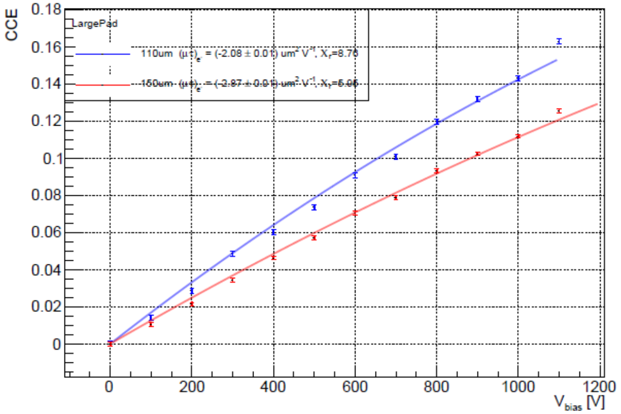

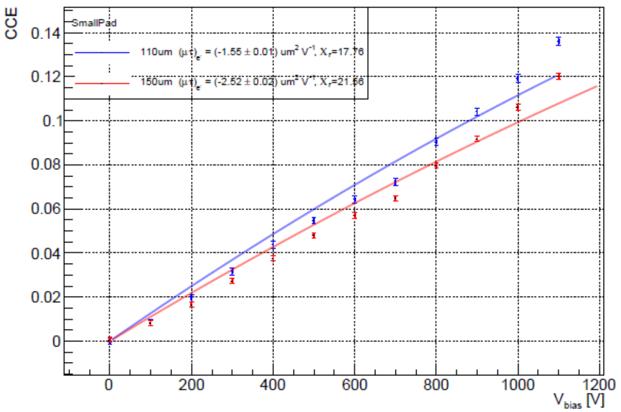

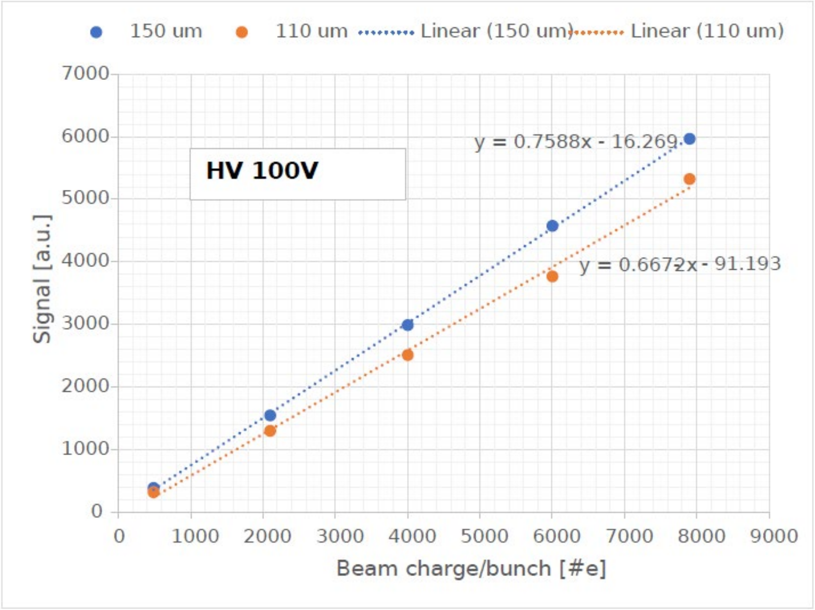

Figure 9.9: Behaviour of the collected charge from the large pad as a function of the beam multiplicity, at a fixed bias voltage of $V_{bias} = 100V$.

Test beams. Four-strip sensor. Scope and setup

- Tomsk 4-strip (80µm x 1cm) sensors have been tested at CLEAR (CERN) with an e$^-$-beam.
- CLEAR facility able to deliver charges 10pC - 270nC with a bunched electron beam (1-180 bunch/train) with gaussian 1x2 mm^2 profile, at a maximum train repetition rate of 10Hz.
- High beam charge allows measurement of strip signals without any amplification, directly at the strip with an oscilloscope.

Investigated

1. Charge collection efficiency vs. HV-bias
2. Strip-response vs. beam position on the strip
3. Relative charge collected after high irradiation (15MGy)

Nb. channels	4	4	3 (1 not working)
Thickness	110um	150um	150um
Manufacturer	Wuppertal	University	M-type
Beam intercept	first	second	third

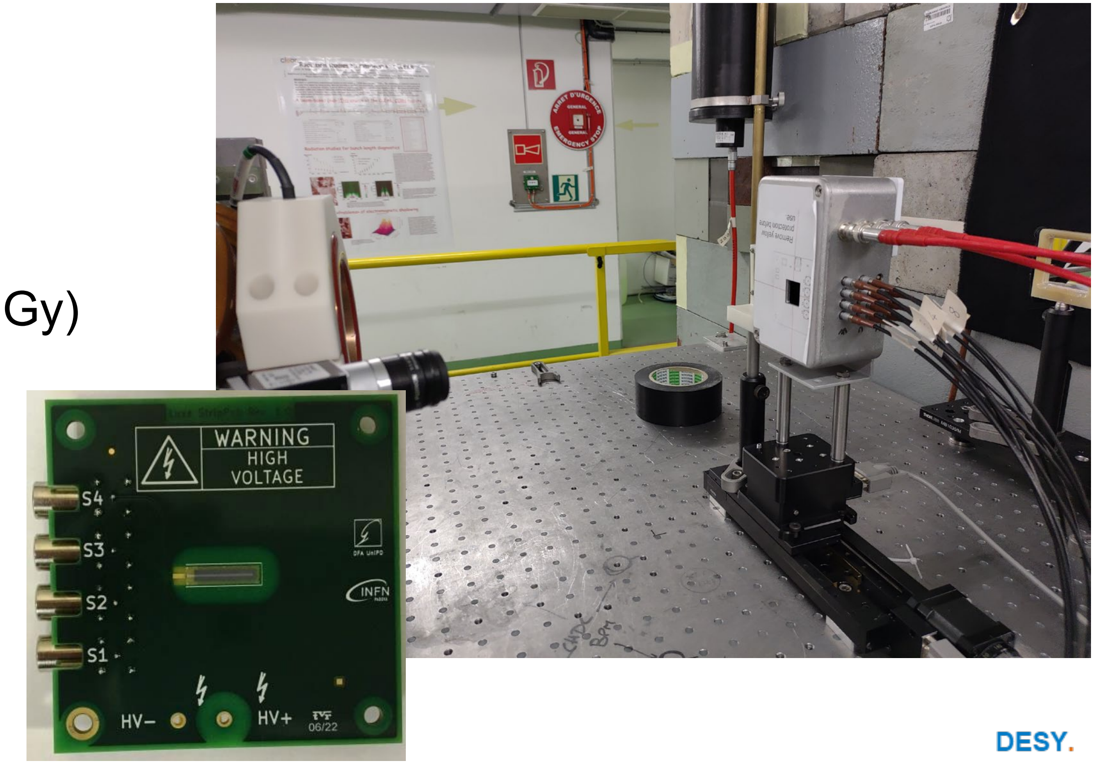

Test beams. Four-strip sensor. Challenges and results

- **Challenges**
  - Facility’s issues at the TB beginning (klystron failures).
    - ► Beam instability (position, width)
    - ► Beam bunch time profile instability after klystron trips
  - Continuous beam profile acquisition (from YAG:Ce) unavailable.
  - Wrong configuration of digitizers in some runs.
  - Wrong timing of beam charge / digitizer data streams, required re-synchronization afterwards.

- **Results**
  - Measurement of the signal produced in sapphire.
  - Sensor uniformity response verified.
  - Relative CCE with irradiation behaviour.

- **Lessons learned**
  - Small strip area requires precise beam profile and charge information shot-by-shot → (scintillator + camera) system

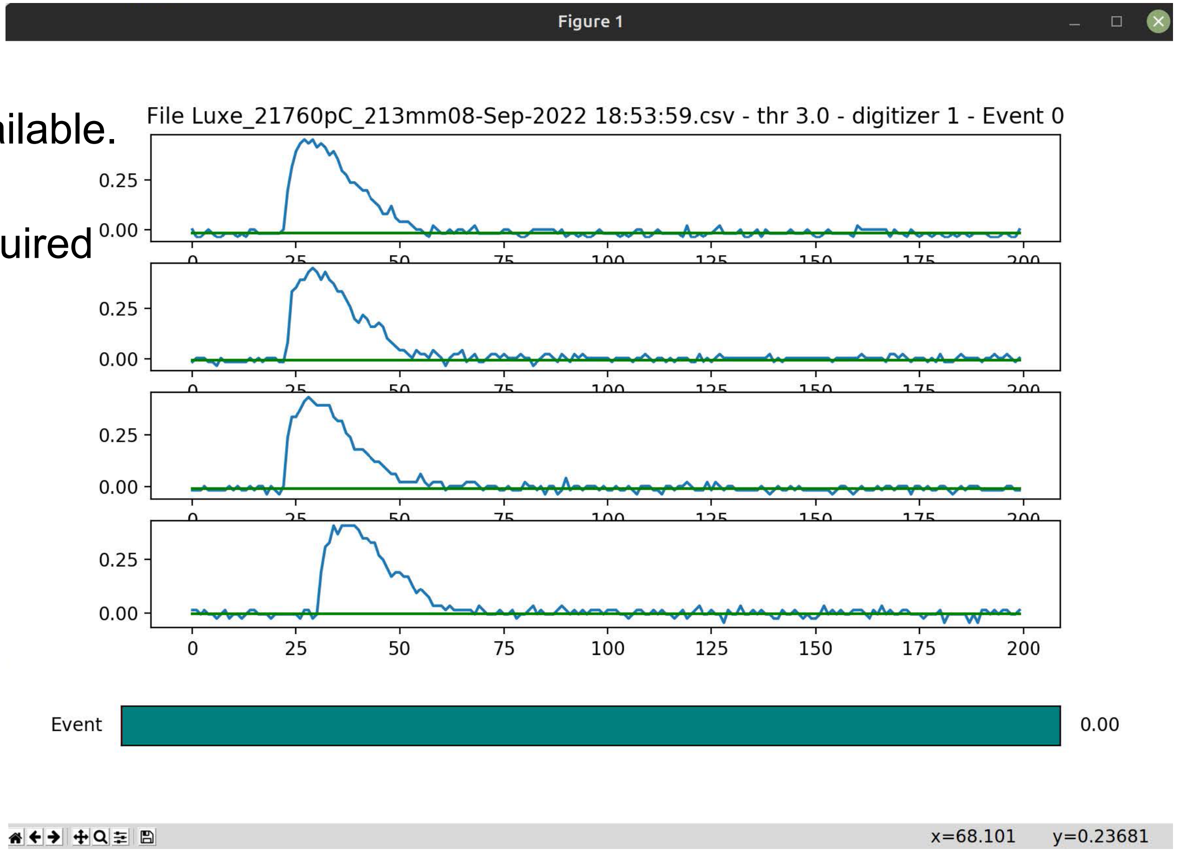

Test beams. GBP sensors. Scope and setup

- Tomsk 192-strip (100µm pitch, 110µm-thick) sensors received Summer ’22.
- Wire bonding made in Pisa, Italy.
- Tested at CLEAR (CERN) with an e$^-$-beam. March ‘23.

- **Goals**
  - First test of the electronics (PS, FERS).
  - CCE(V), CCE(Q) and strip-response with beam pos.
  - Relative CCE w.r.t. the dose delivered (up to 10MGy).
  - BP reconstruction w.r.t. the scintillator screen.
  - Signal/noise w.r.t. different grounding conf.s

- **Setup**
  - 2x192-strip 110µm-thick sensors (University, Monocrystal).
  - Ribbon shielded cables 3m used.
  - Patch panel with 64ch/32ch sensor readout by 2xFERS A5202 cards.
  - Beam profile monitored with a scintillator and a camera, and beam charge acquired event by event.

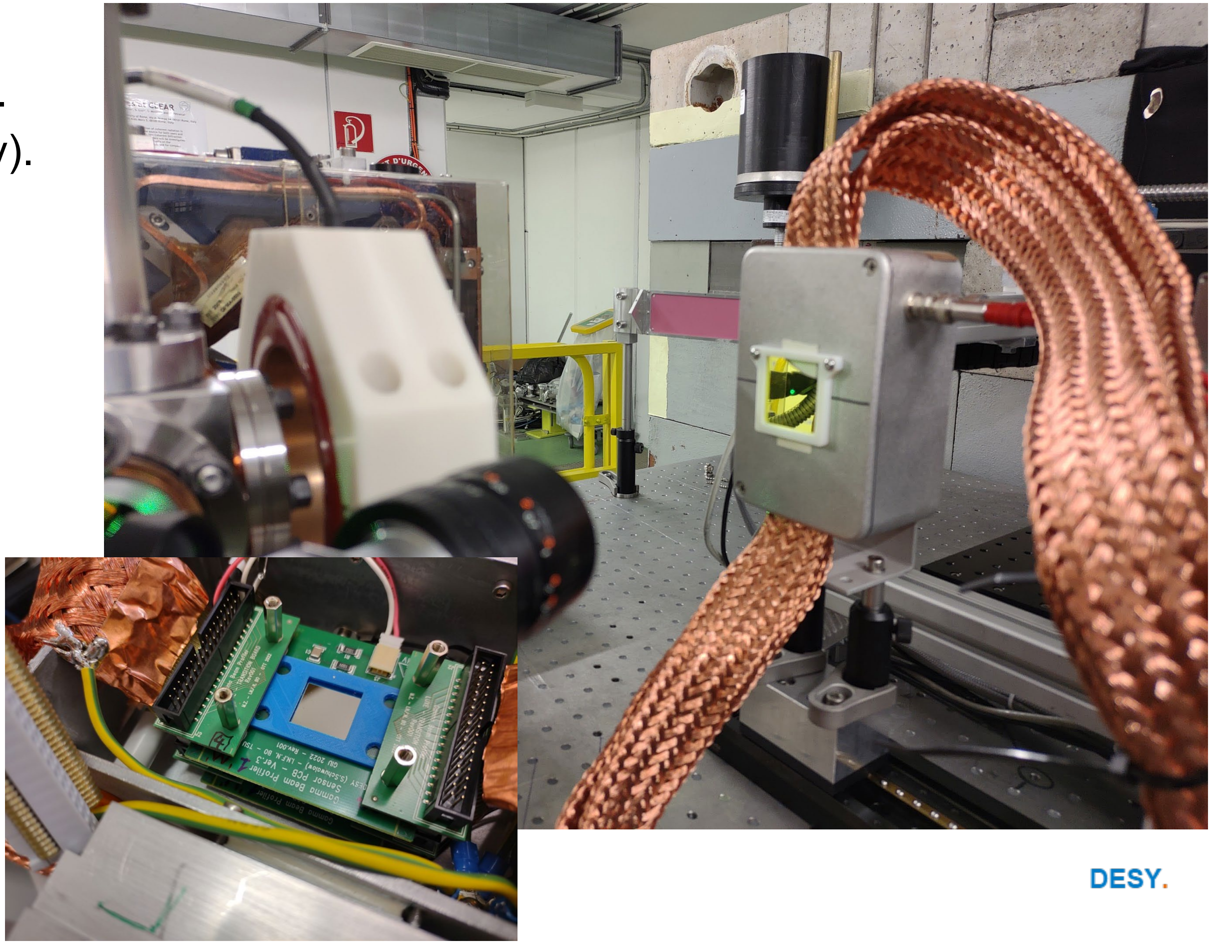

Test beams. GBP sensors. Challenges

- **Challenges**
  - Readout stream from many detectors (sapphire, camera, digitizer, psu, stages) with single PC
  - Time synchronization of the streams

- **Status**
  - Data pre-processing (alignment, synchronization) completed.
  - Data-frame ready for analysis.

- Semi-permanent installation of the GBP at Vesper @ CLEAR (CERN).

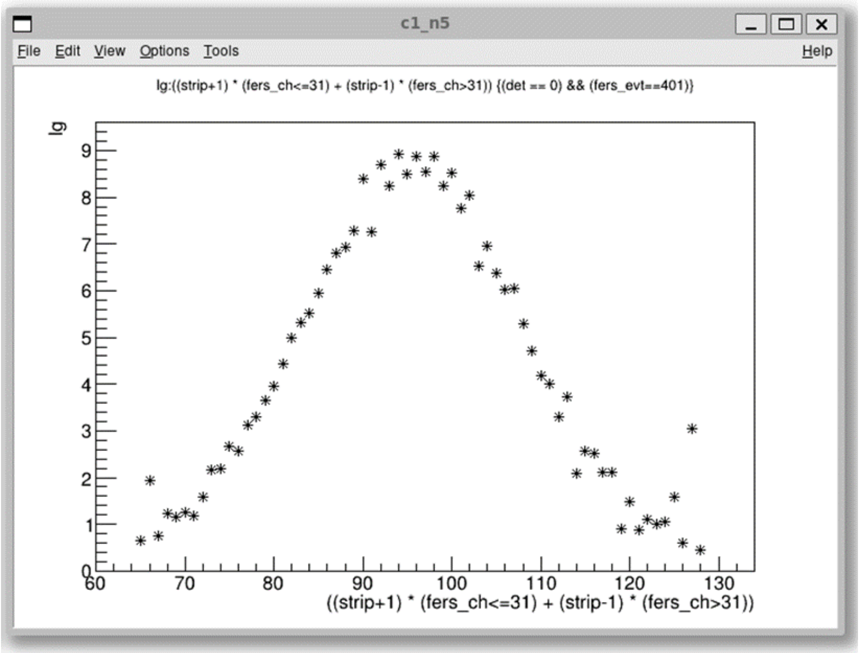

lg:((strip+1) * (fers_ch<=31) + (strip-1) * (fers_ch>31)) {(det == 0) && (fers_evt==401)}